



OPEN ACCESS

EDITED BY

Lena Hirtler,
Medical University of Vienna, Austria

REVIEWED BY

Jiawei Xu,
Massachusetts General Hospital and Harvard
Medical School, United States
Bolun Liu,
Tianjin University of Technology, China

*CORRESPONDENCE

Lin Wang
✉ wlin_xz@163.com

RECEIVED 19 September 2023

ACCEPTED 25 July 2024

PUBLISHED 09 August 2024

CITATION

Wang L, Sun H, Guo K, He K, Geng W, Zhou W
and Wei J (2024) Monte Carlo-based in-depth
morphological analysis of medullary cavity for
designing personalized femoral stem.
Front. Surg. 11:1294749.
doi: 10.3389/fsurg.2024.1294749

COPYRIGHT

© 2024 Wang, Sun, Guo, He, Geng, Zhou and
Wei. This is an open-access article distributed
under the terms of the [Creative Commons
Attribution License \(CC BY\)](https://creativecommons.org/licenses/by/4.0/). The use,
distribution or reproduction in other forums is
permitted, provided the original author(s) and
the copyright owner(s) are credited and that
the original publication in this journal is cited,
in accordance with accepted academic
practice. No use, distribution or reproduction
is permitted which does not comply with
these terms.

Monte Carlo-based in-depth morphological analysis of medullary cavity for designing personalized femoral stem

Lin Wang^{1*}, Hui Sun¹, Kaijin Guo², Kunjin He³, Weizhong Geng⁴,
Wen Zhou¹ and Jian Wei¹

¹School of Medical Information and Engineering, Xuzhou Medical University, Xuzhou, China, ²Department of Orthopedics, Affiliated Hospital of Xuzhou Medical University, Xuzhou, China, ³College of Internet of Things Engineering, Hohai University, Changzhou, China, ⁴College of Computer and Information Engineering, XinXiang University, XinXiang, China

Background: The design of femoral stem prostheses requires a precise understanding of the femoral marrow cavity. Traditional measurements of morphological parameters in the upper femur, particularly the medullary cavity and cortical region, are primarily based on coronal and sagittal axes, which may not fully capture the true three-dimensional structure of the femur.

Methods: Propose a Monte Carlo-based method for a more comprehensive analysis of the femoral marrow cavity, using CT scans of femurs from a selected group of patients. The study aimed to define and calculate anatomically semantic morphological parameters to enhance the understanding of the femoral marrow cavity's anatomical morphological changes, ultimately improving the design and clinical selection of femoral stem prostheses. To enhance the accuracy of femoral stem prosthesis design, this study aims to develop a Monte Carlo-based method for a more comprehensive analysis of the femoral marrow cavity. The proposed method transforms the non-random problem of determining cross-sectional size into a random issue, allowing for the calculation of the size of the medullary cavity and cortical region. Anatomically semantic morphological parameters are then defined, calculated, and analyzed.

Results: The experimental results indicate that the newly defined parameters complement existing ones, providing a more rational scientific basis for understanding the anatomical morphological changes of the femoral marrow cavity.

Conclusion: This research offers essential scientific theoretical support for improved morphologic research, design, and clinical selection of femoral stem prostheses. It holds significant importance and application value in clinical practice, contributing to a more accurate and comprehensive understanding of femoral anatomy for prosthetic design.

KEYWORDS

femoral medullary cavity, region of interest, Monte Carlo method, morphological analysis, femoral stem

1 Introduction

Hip arthroplasty is a surgical procedure in which the hip joint is replaced with a prosthesis to restore the movement of the hip joint (1). A prosthetic hip joint is mainly modeled after the human hip structure. By inserting the femoral stem prosthesis into the femoral marrow cavity of the patient, pain can be relieved while restoring range of

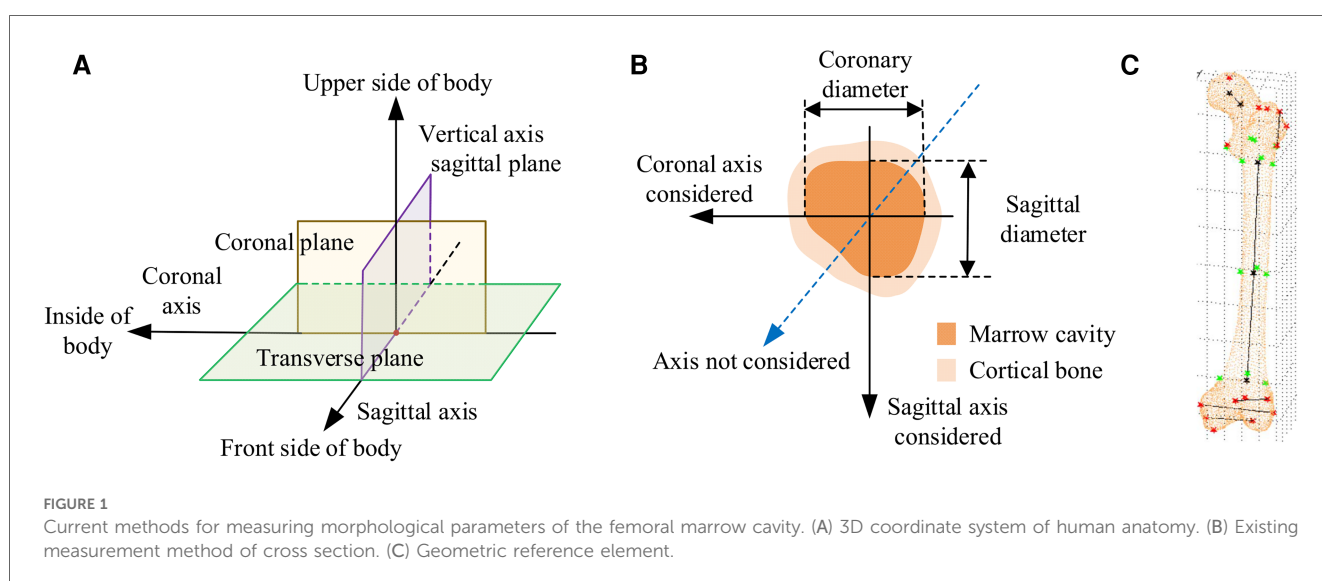
motion and function (2, 3). Despite the continuous advancements in material science, prosthesis design, and surgical techniques, which have significantly reduced the incidence of complications following total hip arthroplasty, it is still not possible to completely avoid the need for revision surgery within five years post-operation (4). Therefore, ensuring the stability of the prosthesis is particularly crucial. Studies indicate that a good match and appropriate size between the femoral stem and the medullary cavity are crucial to achieving adequate initial stability (5), and they also effectively reduce the risk of intraoperative fractures of the femur during implantation (6–8). Consequently, improving the match between the femoral shaft and the medullary cavity has become an urgent issue to be addressed in hip surgery (9). However, the current situation is that the existing specifications and types of femoral stems are limited, and they cannot fully accommodate the needs of all patients. In clinical practice, there are still cases where inadequate anatomical matching between the prosthesis and the recipient bone leads to surgical failure (10–12).

Studies have shown that morphological parameters of the femoral marrow cavity are crucial to the design of the femoral stem (13, 14). Precise measurement and analysis of these morphological characteristics can enhance the adaptability, stability, and durability of femoral stem prostheses (15, 16). Therefore, in order to design a femoral stem prosthesis with the appropriate shape and size, it is necessary to conduct precise analysis of the femoral marrow cavity. However, the morphological characteristics of the femoral marrow cavity vary with age, gender, and region, among other factors (17, 18). This complexity has driven the development of various methods for measuring the morphological features of the femoral marrow cavity. For example, Zou et al. (19) used spiral CT to scan the entire length of the femur, studying the diameter and geometric shape of the marrow cavity in the upper femoral segment, which provided a basis for designing artificial femoral stems for the morphology of the Chinese population. Xue et al. (20) studied the statistical law of the geometric shape of the cross-section of the

upper femoral marrow cavity and automatically extracted the cross-sectional shape of the upper femoral marrow cavity using computer image processing techniques, proposing a parametric mathematical method of conic curve fitting. However, although computer image processing methods can automatically extract the cross-sectional morphology of the marrow cavity and reduce human error, they may require complex algorithms and precise parameter settings. Additionally, computer-based measurement methods may not be applicable to all regions of the marrow cavity, especially in cases of abnormal or irregular morphologies.

In CT images, the normal anatomical morphology of the femoral marrow cavity shows a gradual decrease in diameter from proximal to distal, taking on a trumpet shape rather than a regular round shape. As illustrated in Figures 1A,B, current measurement procedures (21–26) have mainly focused on the coronal and sagittal axes, guided by anatomical markers (27, 28) as shown in Figure 1C. However, this approach ignores other axes, and measurement along the coronal or sagittal axes alone cannot fully or accurately reflect the true three-dimensional morphology of the femoral marrow cavity. Therefore, there is an urgent need for practitioners to gain a comprehensive understanding of the femoral marrow cavities in multiple dimensions.

In CT images, as shown in Figure 1B, the region of interest of the medullary cavity (referred to as ROIMC) includes the marrow cavity and the cortical bone area. The color contrast between the compact and spongy bone of the femur is strong, and the boundary between them is clearly visible. This makes it easy to extract the marrow and cortical regions. The size of these irregular areas can be used as the basic unit to describe the cross-sectional morphology of the femoral marrow cavity. The Monte Carlo method has advantages in resolving the size of irregular areas. It is a computer numerical calculation method based on statistical sampling theory, which estimates and describes the statistics properties of functions through statistical sampling or random simulation of variables, and provides approximate solutions to problems (29). Due to its simple program structure, flexible



simulation process, and adaptability in solving multidimensional problems, this method has been applied in many fields, including physics, engineering, and computer science. In clinical medicine, there have been reports of the application of the Monte Carlo method in calculation of radiation dosages (30). Kirby et al. (31) used the Monte Carlo method to generate a representative digital model that simulated the microstructural of trabecular bone. Eberlea et al. (32) established a non-destructive musculoskeletal simulation model based on kinematic data and used the Monte Carlo method to simulate non-contact anterior cruciate ligament injuries in the knee. Wang et al. (33) reported the use of an adaptive Monte Carlo method in top-down measurement assessment. By using the adaptive Monte Carlo method (aMCM), this study verified the effectiveness of the top-down method in the assessment of clinical laboratory uncertainties, which provides important theoretical support for the precise measurement of the femoral marrow cavity discussed in this study.

Based on years of research results obtained by our working group (34–36), this paper presents a Monte Carlo-based in-depth morphological analysis of the medullary cavity. Main work includes the extraction of the femoral ROIMC, Monte Carlo simulation of ROIMC, and calculation and analysis of femoral marrow cavity morphology. The research work can be used as a supplement to the existing research results, and therefore provide more reasonable scientific basis for comprehensively understanding the anatomical morphological changes of the femoral marrow cavity. Meanwhile, our research provides the necessary scientific theoretical support for improved morphologic research, design, and clinical selection of femoral stem prostheses and has important significance and application value in clinical practice.

The structure of the remainder of this study is as follows. Section 2 outlines the data sources and research methodology employed. Section 3 evaluates the reliability of the method proposed in this paper. Section 4 presents the experimental results. Section 5 discusses the findings. Finally, Section 6 concludes the study and suggests directions for future research.

2 Materials and methods

2.1 Data acquisition

The methodology presented in this work was verified using CT scans of femurs. In preparation, a total of 10 patients during 2019–2020 were voluntarily enrolled. Approval from the Ethics Committee of Xuzhou Medical University was obtained. Patients meeting one of the following requirements were excluded from our study: (1) individuals with a history of therapies that might potentially affect bone mass, structure; (2) women who were pregnant, breastfeeding, or who were planning to get pregnant; and (3) individuals with genetic relationships, such as parent-child or sibling relationships. After informed consent was obtained and associated risks were explained, their age, sex, height, medical history, and physical activity were obtained.

The CT images of these patients were scanned under the professional guidance of the clinician. Proper patient positioning

is crucial for obtaining high-quality images in a CT scan. In this study, the patient was positioned as follows: The patient was supine in the center of the CT bed, with both lower limbs rotated in the neutral position and maintained in the standard anatomic position. To prevent the patient from moving during the scan, a mat was used to help keep the patient in position. Light Speed VCT helix scan, produced by GE, was used. The main parameters were as follows: tube voltage 120 kV; tube current 300 mA; layer thickness 0.6 mm; layer spacing 5.0 mm; scanning time 1.5 s. To facilitate parameter measurement, the imaging axis during the scan is set as follows: The imaging axis is defined relative to the patient's anatomy and the orientation of the CT beam. The main axis, shown in Figure 1A, is sagittal, dividing the body into left and right halves is sagittal from front to back, dividing the body into left and right halves. The coronal axis runs from side to side, dividing the body into anterior and posterior parts. The horizontal axis runs horizontally, dividing the body into upper and lower parts.

2.2 Methods

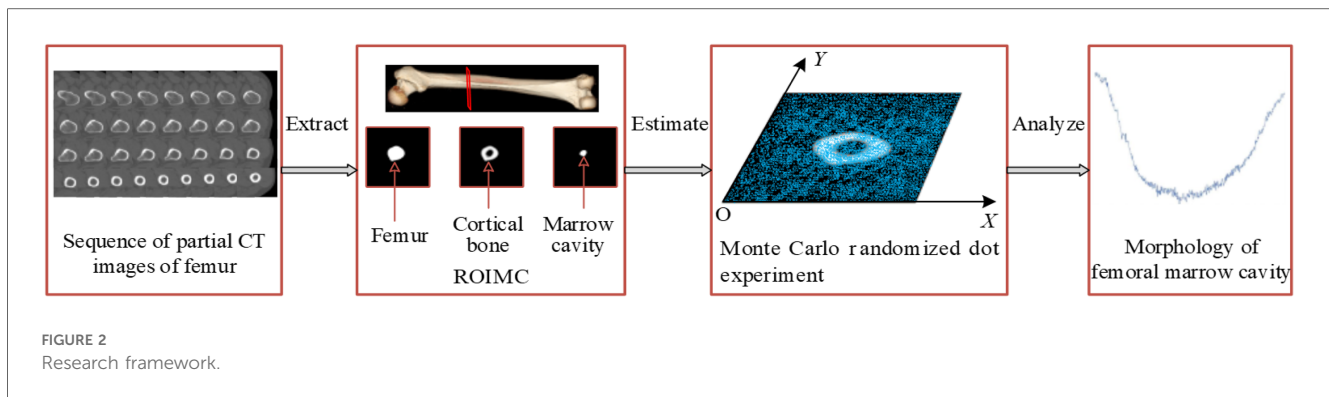
To obtain a more comprehensive understanding of femoral marrow cavity morphology and to improve the design quality of customized femoral stems, a morphological parameter analysis method based on Monte Carlo is proposed, as shown in Figure 2. The main steps of this framework are as follows:

- Step 1: extract the ROIMC of the femur. The femoral marrow cavity and cortical bone region are extracted based on binarization, contour extraction, image subtraction, and other operations.
- Step 2: calculate ROIMC statistics. According to the extracted medullary cavity and cortical bone, the statistics of medullary cavity and cortical bone are estimated based on Monte Carlo randomized dot experiment.
- Step 3: define and calculate the morphological parameters of femoral marrow cavity. Taking the ROIMC as the basic unit and combining it with clinical needs, the morphological parameters of femoral marrow cavity are calculated.

2.2.1 Extraction of ROIMC

The ROIMC mentioned in this paper mainly contains the cortical bone and medullary cavity areas on CT images. Considering that CT images are formed by the post-decay of electromagnetic rays through the human body, resulting in the presence of isolated pixel points or blocks with strong visual effects, unclear edge contours, and sharp changes in regional gray levels. Furthermore, the gray level of femur CT images is relatively complex, which increases the difficulty of contour extraction. Therefore, for denoising, Gaussian filtering is adopted to convolve the 2D Gaussian kernel with the CT femur image so that the value of each pixel can be obtained from the weighted average of its own and other pixel values in the neighborhood.

Gaussian filtering uses the product of two 1D Gaussian functions in the x and y dimensions, with their respective



standard deviations, σ_x and σ_y , being equal. The formula is as follows:

$$\begin{cases} G(x, y) = \frac{1}{2\pi\sigma^2} e^{-(x^2+y^2)/2\sigma^2} \\ u = u_x = u_y \\ \sigma = \sigma_x = \sigma_y \end{cases} \quad (1)$$

On the basis of noise removal, the pixel value greater than the threshold is retained, while those with values less than the threshold, T_0 , are set to zero, as follows:

$$dst(x, y) = \begin{cases} src(x, y) & src(x, y) > T_0 \\ 0 & \text{otherwise} \end{cases} \quad (2)$$

Additionally, while the high contrast between the cortical bone and the medullary cavity in CT imaging aids in distinguishing these structures, determining their precise boundaries remains challenging. To reduce potential biases, we employed the well-established Canny edge detection algorithm (37). This algorithm effectively eliminates some interference while precisely locating image edges. It achieves this by suppressing non-maximum values in the image and using a double-threshold approach for edge detection, which reduces the rate of edge misjudgment, sharpens the edges, and suppresses the appearance of false edges. In our experiments, we utilized the Canny operator, and the effect of boundary extraction on key slices is shown in Figure 3. By employing these methods, we have minimized biases that might arise in CT imaging studies, thereby enhancing the credibility and accuracy of our research findings.

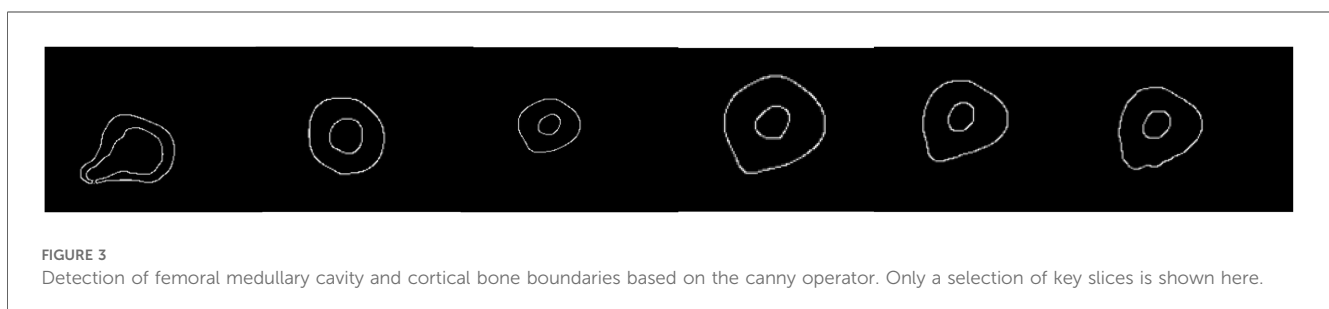
Owing to the complexity of femoral CT images and the great influence of noise, by comparing the pixel values, contrast sizes, and actual characteristic information of different CT images in the femoral part, based on the precondition of ensuring the anti-noise effect and information integrity, σ and T_0 are determined. The image is divided into different areas with gray characteristics by setting the appropriate gray threshold, and the cortical bone and medullary cavity are extracted through a series of operations, such as contour extraction and subtraction. The extraction result is shown in Figure 4.

2.2.2 Calculation of ROIMC statistics

Monte Carlo method establishes an appropriate probability model or a random process, set its parameters equal to the solution of the problem, and repeat sampling experiments until one obtains statistical analysis of the results. Monte Carlo method has unique advantages when solving a solution in an irregular region. Using the Monte Carlo method for calculating lake area is a very typical example. The area of the lake is determined from the number of balls fired randomly from a cannon that land in the lake. In relative terms, higher the number of balls fired is, better the estimation of the lake area is. Thus, the area of the lake is directly proportional to the number of balls that land in the lake. As is shown in Figure 5, the size of the lake (S_{target}) is expressed as

$$S_{\text{target}} = S_{\text{full}} \cdot \frac{M_{\text{target}}}{M_{\text{full}}} \quad (3)$$

where S_{full} represents the size of the entire area, M_{full} represents the total number of balls, and M_{target} represents the number of balls that land in the lake.



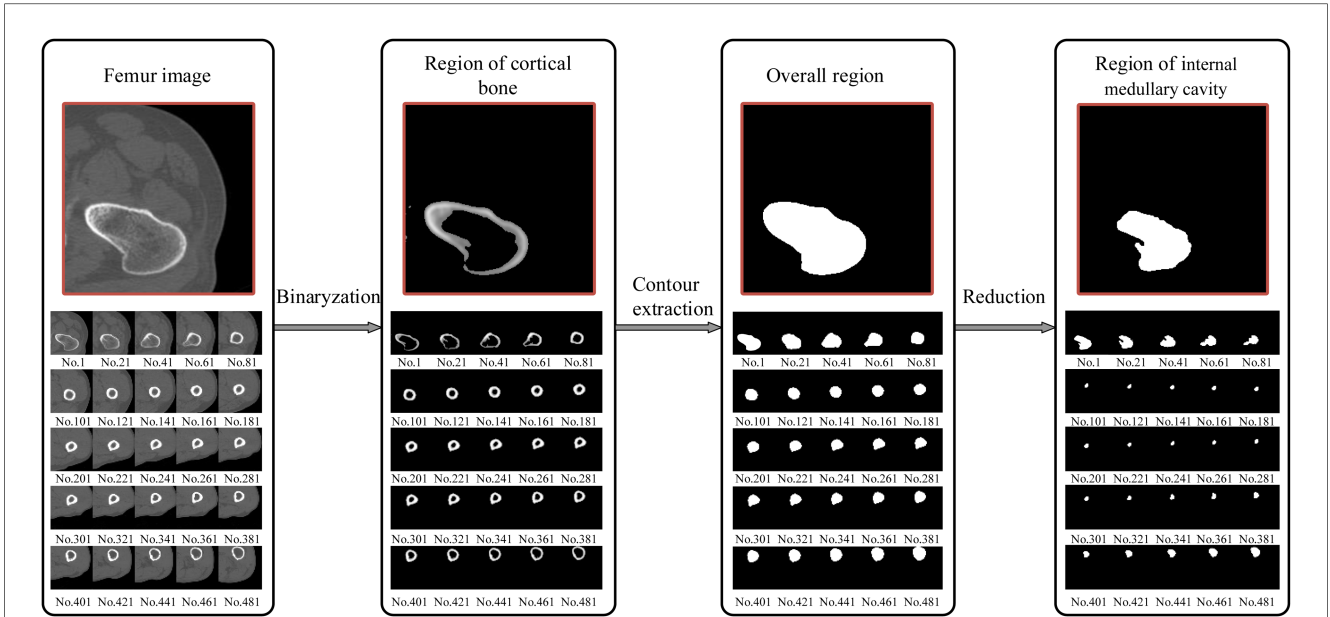


FIGURE 4 Extraction of the femur region of interest (ROI); from the proximal end to the distal end, one of every 20 CT images is selected. The final window size is 7×7 , with a standard deviation (σ) of 3 and a threshold (T_0) of 117. The size of the internal medullary cavity area, referred to as s_m , describe the medullary cavity area in the transverse section. Similarly, the cortical area, effered to as s_c , describe the size of the cortical region in the transverse section.

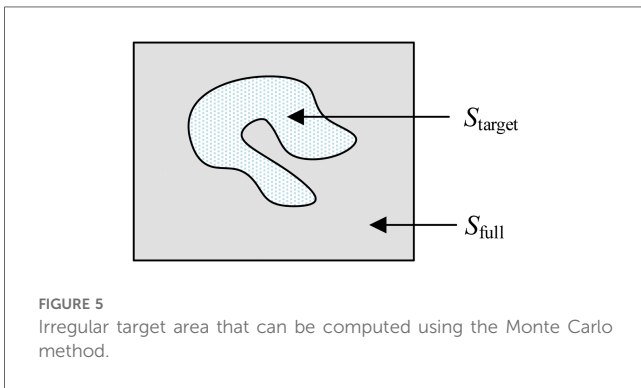


FIGURE 5 Irregular target area that can be computed using the Monte Carlo method.

In this paper, a probability model is established to describe the ROIMC in the form of statistics, and its estimated value is obtained via experimental simulation and mathematical statistics. As shown in Figure 6, s_m and s_c of a cross section of the diaphysis region, the main steps are as follows:

- Step 1: set a rectangle of the same size as the femur CT image. The long side of the rectangle, a , is used as the x -axis, and the short side, b , is used as the y -axis to establish a Cartesian system. a and b are expressed in pixel. The intersection point of the long and short sides is the origin, o , of the coordinate system.
- Step 2: conduct a simulation experiment. Random points having a uniform distribution of X and Y on $[0, a]$ and $[0, b]$, respectively, are generated in the rectangular region. The number of points falling into the area contained in the lateral boundary curve of the cortical bone (femoral overall area, white area in Figure 6A) is n_1 , and the number of points not falling into the

cortical bone area (white area) is n_2 . Thus, the number of points falling into the cortical bone area in Figure 6B and the white medullary cavity area in Figure 6C are $n - n_2$ and $n_1 - (n - n_2)$, respectively. Assuming that the proportion of cortical bone region to rectangular region, α_c , and the proportion of medullary cavity region to rectangular region, α_m , is calculated as follows:

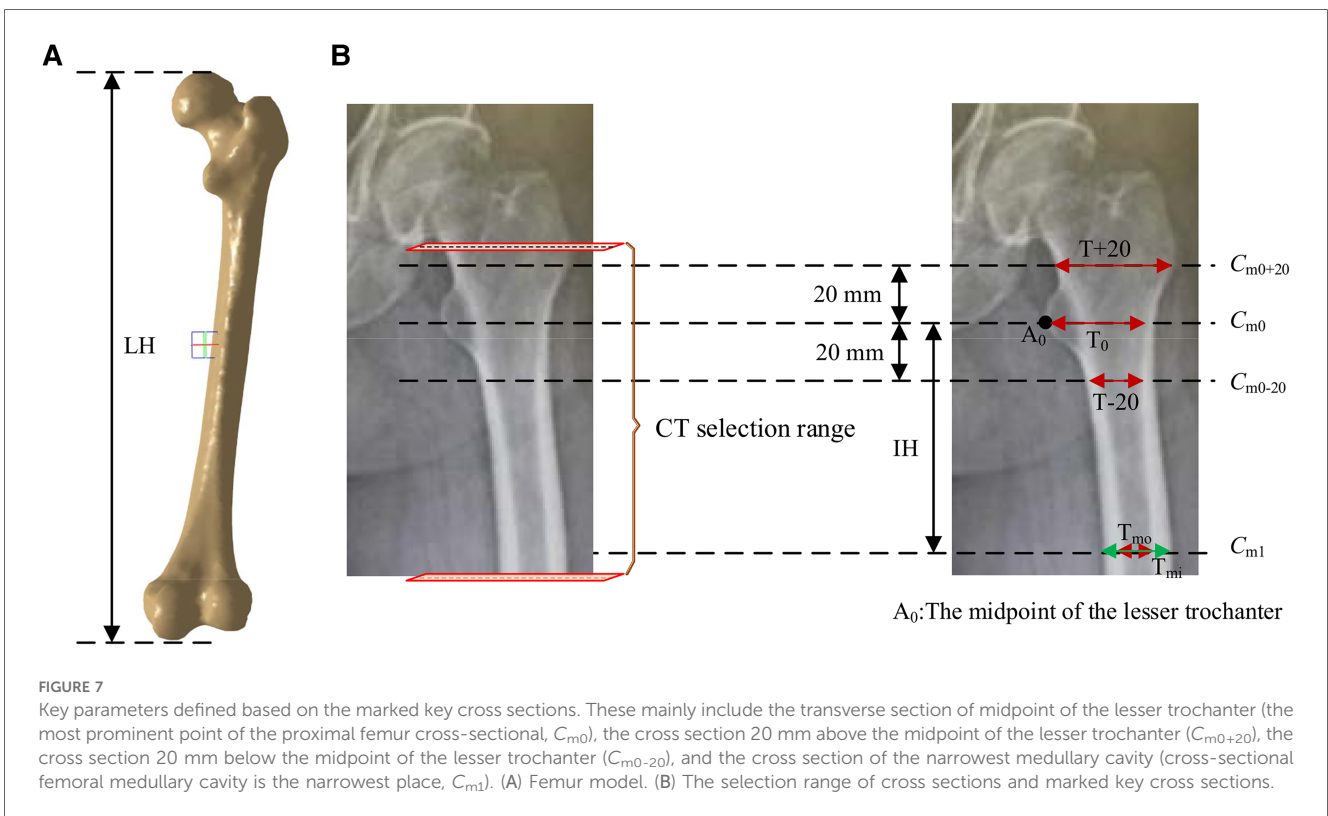
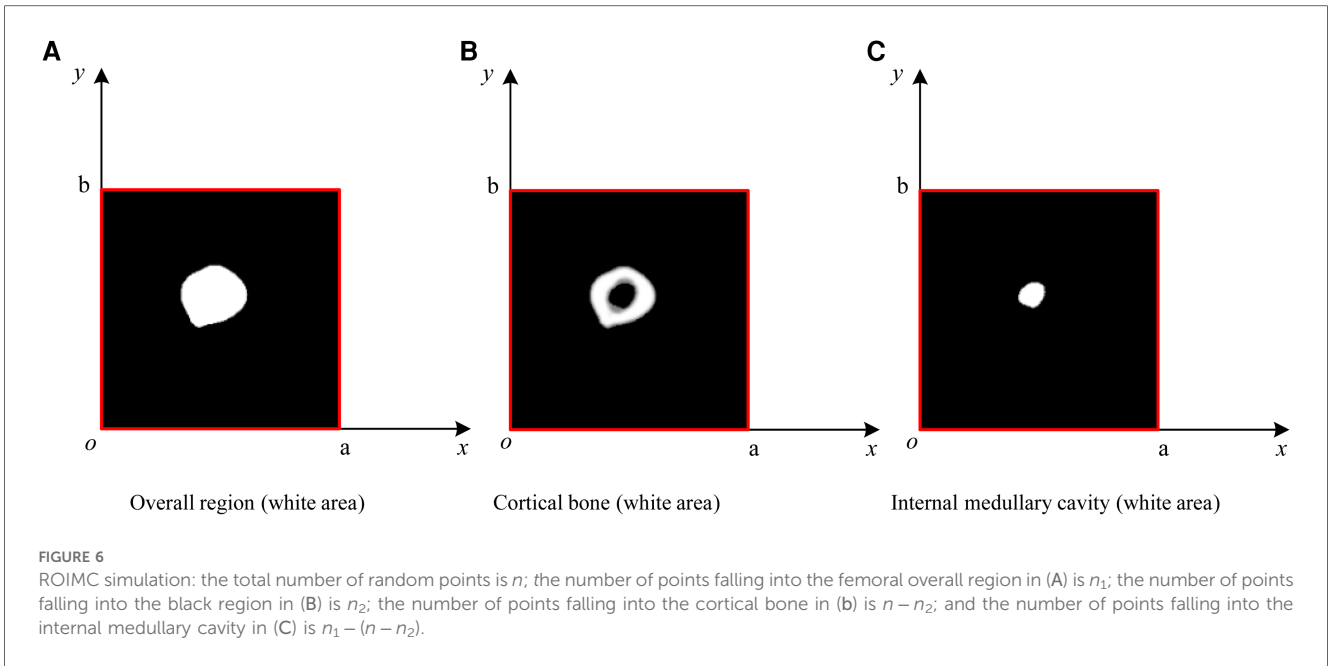
$$\begin{cases} \alpha_c = (n - n_2)/n \\ \alpha_m = (n_1 - (n - n_2))/n \end{cases} \quad (4)$$

Step 3: the estimated value of the cortical bone region, s_c , and the medullary cavity region, s_m , in the transverse section of the femur are calculated as follows:

$$\begin{cases} s_c = \alpha_c \times a \times b \\ s_m = \alpha_m \times a \times b \end{cases} \quad (5)$$

2.2.3 Definition of morphological parameters

According to the requirements of the design of femoral prosthesis stem, it is necessary to combine clinical experience and data analysis to determine the range of CT data and the cross section of markers (38). As shown in Figure 7, in order to more accurately determine the cross section of the marker, it is necessary to expand the selection of more CT ranges. In addition, the labeling of key transverse sections is very important for the measurement of femur morphological parameters. The key sections of this paper refer to Noble's research (39).



According to the existing morphological parameters of the medullary cavity (18–22), the parameters listed in Table 1 are included in the calculation range. These parameters are roughly divided into three types: diameter parameters, length parameters and ratio parameters. The diameter parameters include the medullary internal diameter 20 mm above the lesser trochanter ($T + 20$), the medullary internal diameter 20 mm below the lesser

trochanter ($T + 20$), the medullary internal diameter at the lesser trochanter (T_0), the medullary internal diameter at the isthmus (T_{mi}) and the medullary outside diameter at the isthmus (T_{mo}). These parameters can be calculated based on key cross sections marked in Figure 7. The length parameters include isthmus height (IH) and the length of the femur (LH). The ratio parameters include the canal flare index (CFI), metaphyseal canal

TABLE 1 Commonly used single-axial morphological parameters of personalized femoral marrow cavity.

Types	Parameters	Description (unit of the length parameter: mm; unit of the ratio parameter: 1)
Diameter parameters	$T + 20$	Medullary internal diameter 20 mm above the lesser trochanter
	$T - 20$	Medullary internal diameter 20 mm below the lesser trochanter
	T_0	Medullary internal diameter at the lesser trochanter
	T_{mi}	Medullary internal diameter at the isthmus
	T_{mo}	Medullary outside diameter at the isthmus
	T_c	The thickness of the cortical bone, with a thickness value on each slice.
Length parameters	IH	Isthmus height, the vertical height between the transverse plane where the center of the lesser trochanter is located and the transverse plane of the isthmus
	LH	The length of the femur, vertically, and the height between the highest and lowest point of the femur.
Ratio parameters	IH/LH	The ratio of IH to LH
	CFI	Canal flare index, and its value is equal to $T + 20/T_i$
	MCFI	Metaphyseal canal flare index, and its value is equal to $T + 20/T - 20$
	DCFI	Distal canal flare index, and its value is equal to $T - 20/T_i$
	CI	Cortical index, and its value is equal to $(T_{mo} - T_{oi})/T_o$

flare index (MCFI), distal canal flare index (DCFI), and cortical index (CI). These parameters are an important basis for the design of femoral stem prosthesis.

In addition to the common morphological parameters listed in Table 1. According to the existing design requirements of femoral shaft prostheses, this paper defines the morphological parameters shown in Table 2. These parameters mainly include:

- (a) s_c , the size of cortical area, describe the size of cortical region in transverse section.
- (b) s_m , the size of the internal medullary cavity area, describe the of medullary cavity area in transverse section.
- (c) q_1 , the ratio of the internal medullary cavity to the femoral overall region, describe the ratio of internal medullary cavity to femoral region on cross section.
- (d) q_2 , the ratio of the internal medullary cavity to the cortical bone, describe the ratio of the internal medullary cavity to cortical bone region on cross section.
- (e) r_1 , the growth rate of internal medullary cavity of the lesser trochanter, which describes the growth rate of internal medullary cavity region between C_{m0-20} and C_{m0+20} . s_{m0-20} and s_{m0+20} represent sizes of internal medullary cavity area (pixel) at C_{m0-20} and C_{m0+20} .
- (f) r_2 , the growth rate of the internal medullary cavity of the upper femoral shaft, describes the growth rate of internal medullary cavity region between C_{m1} and C_{m0+20} . s_{m1} and s_{m0+20}

represent sizes of internal medullary cavity area (pixel) at C_{m1} and C_{m0+20} .

These parameters can be used to comprehensively examine all the dimensions of the femoral cross section and can reveal the change rule of the femoral marrow cavity from proximal to distal ends in a more comprehensive, detailed, and vivid way.

3 Rater reliability evaluation

Each patient’s CT scan consists of over a thousand images. To verify the effectiveness and reliability of our method’s computations on each slice, it is sufficient to select a single patient for validation. In this verification experiment, we chose a 50-year-old Han male patient with a height of 175 cm.

According to the design requirements of the femoral stem prosthesis, 492 DICOM format images (refer to the ranges marked in Figure 6B) were selected as experimental data. A Monte Carlo point experiment was implemented using Python v3.3 on a Windows-10 platform. The number of random points was 230,400, and its X and Y coordinates were integers between 0 and 239. Parameters shown in Table 4 were measured using Mimics v15.0 software. The processor was an Intel® Core™ i7-950H processor at 2.60 GHz, and the memory was 8 GB. SPSS v24.0 statistical software was used for statistical processing of the experimental data.

To verify the accuracy of the Monte Carlo method, it was compared to the traversal method. In this experiment, traversal method refers to that each pixel in the target area of interest was accessed once and only once in turn along a search route. The target area of interest contains cortical bone and medullary cavity region. Two groups of parameters are compared. One group was α_{cm} and α_{ct} , the proportion of cortical bone pixels in the whole CT image calculated by Monte Carlo method and traversal method, respectively. And the other group was α_{mm} and α_{mt} , the proportion of medullary cavity pixels in the whole CT image calculated by Monte Carlo method and traversal method, respectively. The statistical

TABLE 2 Morphological parameters of femoral marrow cavity.

Parameters	Description	Express formula
s_c	Size of cortical area (pixel)	$s_c = \alpha_c.a.b$
s_m	Size of internal medullary cavity area (pixel)	$s_m = \alpha_m.a.b$
q_1	Ratio of internal medullary cavity to femoral overall region	$q_1 = s_m/(s_c + s_m)$
q_2	Ratio of internal medullary cavity to cortical bone	$q_2 = s_m/s_c$
r_1	Internal medullary cavity growth rate of small trochanter	$r_1 = (s_{m0+20} - s_{m0-20})/s_{m0-20}$
r_2	Internal medullary cavity growth rate of upper femur	$r_2 = (s_{m0+20} - s_{m1})/s_{m1}$

TABLE 3 Statistical description of α_{mm} , α_{mt} , α_{cm} , and α_{ct} .

	Total layers	Average	Standard deviation	95% CI for the mean		Minimum value	Maximum
				Lower limit	Upper limit		
α_{mm}	492	0.021415	0.0180375	0.019817	0.023013	0.0072	0.0809
α_{mt}	492	0.021417	0.0180652	0.019816	0.023017	0.0076	0.0809
α_{cm}	492	0.043364	0.0052359	0.042901	0.043828	0.0358	0.0586
α_{ct}	492	0.043363	0.0052236	0.042900	0.043826	0.0360	0.0584

TABLE 4 ANOVA of α_{mm} and α_{mt} , and α_{cm} and α_{ct} .

Coefficient		Sum of squares	Degrees of freedom	Mean square	Significant
α_{mm} and α_{mt}	Intergroup	0	1	0	0.999
	Intra-group	0	1	0	0.999
		0.320	982	0	/
α_{cm} and α_{ct}	Intergroup	0	1	0	0.996
	Intra-group	0	1	0	0.996
		0.027	982	0	/

descriptions of these parameters are shown in Table 3. Figure 8 shows the changes of these parameters on different layers. As can be seen from Table 3 and Figure 8, the results obtained by the Monte Carlo method are basically the same as those obtained by the traversal method.

To further verify the correctness of this conclusion, a single-factor ANOVA test was adopted, and the results are shown in Table 4. As can be seen, the significance levels of α_m and α_c obtained by the Monte Carlo and traversal methods was 0.999 and 0.996, respectively, when the significance level of 0.05 was selected. This indicates that there was no significant difference between the two datasets. Therefore, using the Monte Carlo method to calculate ROIMC is reliable and feasible.

4 Results

4.1 Common morphological parameters

The built-in Measure Distance function in Mimics 15.0 (Materialize, Leuven, Belgium) (accuracy: 0.01 mm) was used to record the medullary internal diameter parameters shown in Table 1, and each measurement was repeated three times and then averaged. The diameter parameters as shown in Table 5 were measured as shown in Table 5. Meanwhile, the ratio parameters are also calculated according to the diameter parameters. Additionally, we have listed the corresponding parameter results from literature (19) and (21). It can be observed that the data in this paper are largely consistent with these research findings.

From Figure 9, it can be observed that in the proximal femur, particularly in the metaphysis region, the cortical bone is significantly thinner than in the shaft region. This is consistent with the findings reported in the existing literature (40). This

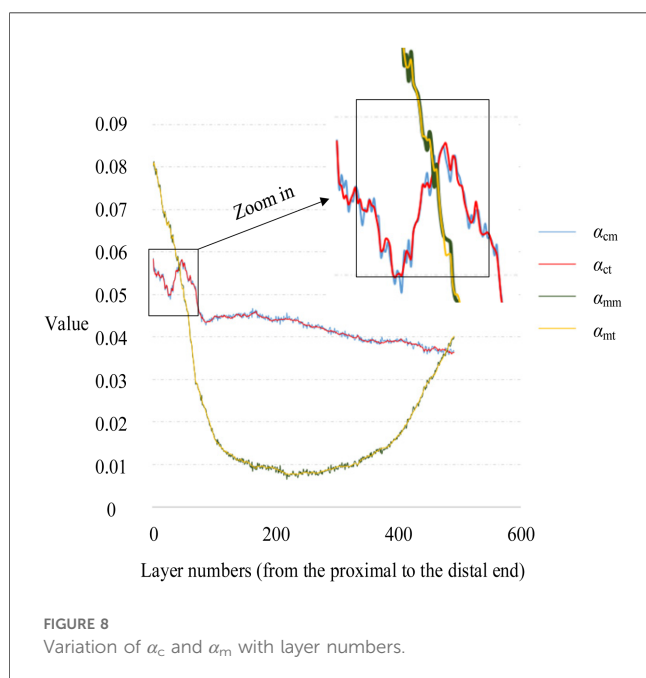


FIGURE 8 Variation of α_c and α_m with layer numbers.

TABLE 5 Commonly used single-axial morphological parameters of personalized femoral marrow cavity.

Parameters	Values			
	Our work	Chen HX (23)	Pi YG (25)	Noble (39)
$T + 20$	43.24	39.9 ± 4.7	43.55 ± 5.26	45.4 ± 3.6
$T - 20$	18.07	17.2 ± 2.9	18.32 ± 2.98	21.0 ± 2.4
T_0	24.40	/	25.47 ± 3.6	29.7 ± 2.9
T_{mi}	10.57	11.3 ± 2.6	10.71 ± 2.26	12.1 ± 1.5
T_{mo}	25.20	/	27.42 ± 2.8	/
IH	110.40	105.0 ± 15.9	106.97 ± 15.92	/
LH	446.96	414.2 ± 31.0	/	/
IH/LH	0.247	0.25	/	/
CFI	4.09	3.70 ± 0.94	4.24 ± 1.00	4.05 ± 0.66
MCFI	2.39	2.36 ± 0.41	2.42 ± 0.35	/
DCFI	1.71	/	1.75 ± 0.31	/
CI	0.58	/	0.61 ± 0.07	0.55 ± 0.05

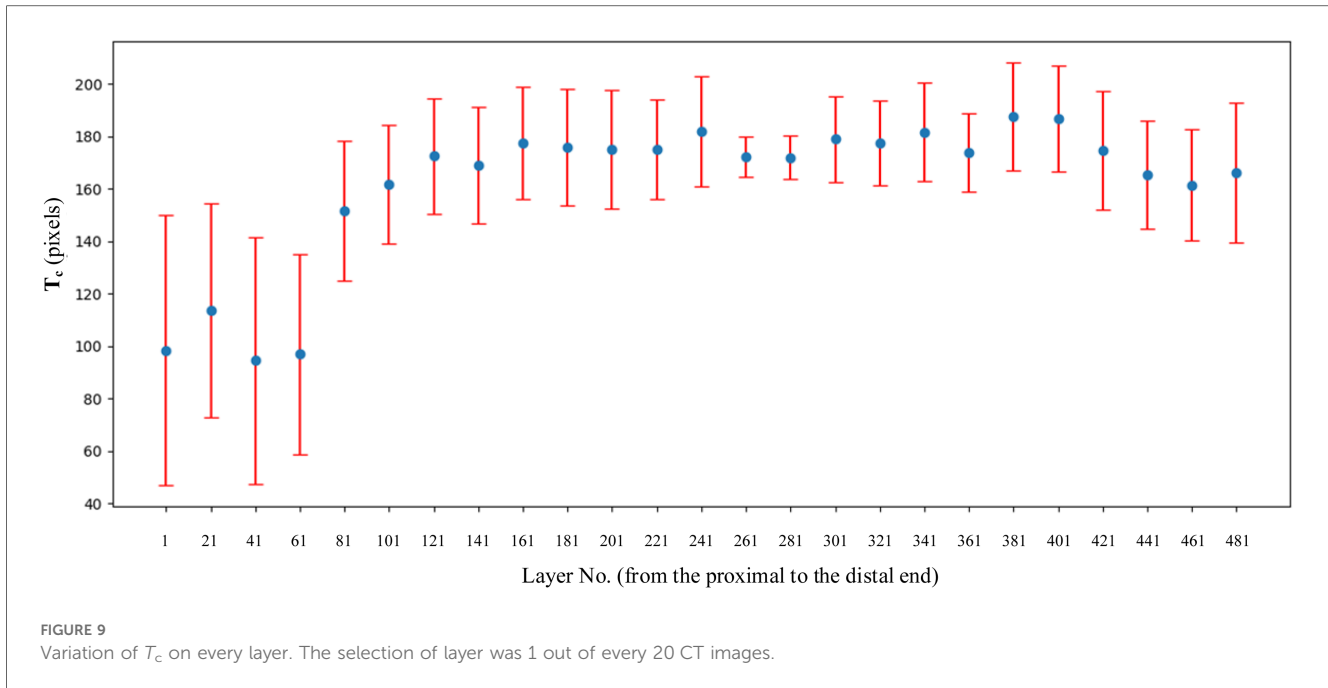


TABLE 6 Morphological parameters of personalized femoral marrow cavity defined in this article.

	Total layers	Minimum value	Maximum value	Average	Standard deviation
s_c	492	2,062	3,377	2,497.79	301.587
s_m	492	412	4,658	1,233.51	1,038.959
s	492	2,868	7,996	3,731.30	1,239.042
q_1	492	0.12	0.60	0.2921	0.13587
q_2	492	0.1418	1.4749	0.478445	0.3490807

indicates that the shape and size of the prosthesis should be adapted to the anatomical structure of the femur, especially to match the morphology of the region with thin cortical bone, in order to prevent prosthesis loosening.

4.2 Morphological parameters defined in our study

Combined with the parameters defined in Table 2, the values of basic intermediate variable parameters used in parameter calculation in Table 2 are shown in Table 6. The statistics for these parameters include the maximum value, minimum value, mean, and standard deviation.

5 Discussion

5.1 Diameter parameters and prosthesis design

As can be seen from Table 5, the values of $T + 20$, $T - 20$ and T_0 in this study were similar to those in references (23) and (25), and were less than those in the Noble (39) group and Rubin (41) group. This discrepancy suggests that when designing prostheses

for patients, reference should not be made to prostheses imported from Western countries, but rather the design should be based on the medullary cavity data of the Chinese population.

Particularly noteworthy is that $T - 20$ and T_0 were significantly smaller than the Noble group (39). The area 20 mm below the lesser trochanter represents the transition zone between the femoral shaft and the metaphysis. Histologically, this region exhibits a transition from spongy to compact bone. Morphologically, there is a marked narrowing at this junction. To allow the femoral shaft to pass through this narrow area and to achieve a press-fit in the proximal metaphyseal region, medullary reaming is usually necessary. However, over-reaming can compromise the load-bearing capacity of the proximally fixed femoral implant. For a medullary canal that is significantly narrowed to a funnel shape at $T - 20$, it is recommended that the femoral stem be designed with a narrower neck-shaft junction and a smaller anteroposterior diameter to ensure proper fit and stability.

Additionally, we are considering whether the differences between our $T - 20$ and T_0 values and those of international groups are a result of using a fixed 40 mm interval as a marker for all subjects. Unfortunately, to date, there have been no reports confirming any negative effects of this fixed 40 mm selection. Therefore, in clinical practice, this method of fixed selection has consistently followed the approach used by Noble. Certainly, without sufficient sample data, it is possible that individual variations may account for such

outcomes. In the future, we may investigate the correlation between medullary cavity parameters and the fixed selection of 20 mm above and below the lesser trochanter.

5.2 Ratio parameters and prosthesis design

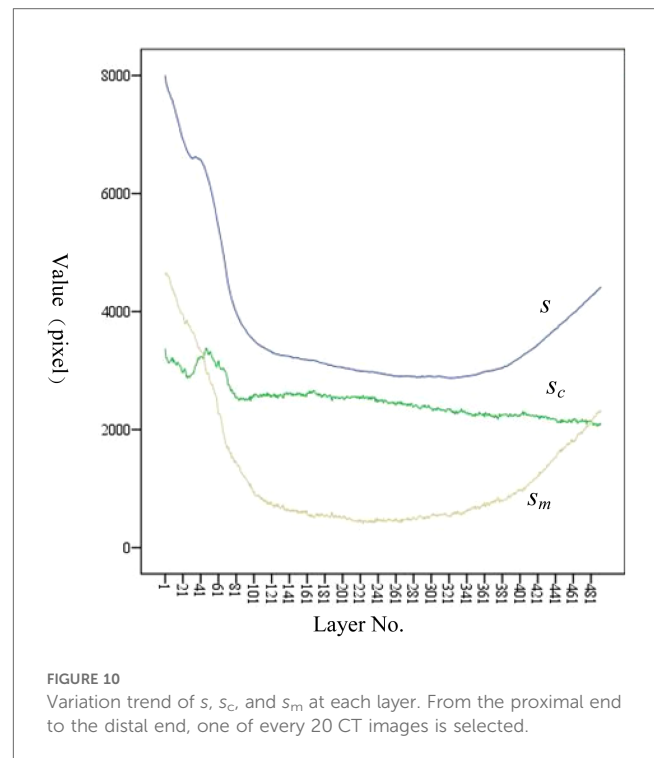
Noble (39), a foreign scholar, proposed for the first time in 1988 to use CFI to describe the shape of the proximal medullary cavity of the femur. They measured and analyzed femur x-rays from 200 normal adults, obtaining a CFI value of 3.8 ± 0.74 . According to the CFI value, the proximal femoral medullary cavity can be divided into chimney ($CFI < 3.0$), normal ($3.0 \leq CFI < 4.7$), and champagne types ($4.7 \leq CFI < 6.5$). Studies indicate that as the elderly age, CFI tends to decrease overall, resulting in a medullary cavity that becomes broader and straighter. Consequently, when designing femoral stem prostheses, preference should be given to larger, distally columnar stems or those with a distally wide rectangular shape. Designing a slender, tapered cylindrical stem at the distal end may make it challenging to achieve the desired three-point fixation, thereby compromising initial stability.

IH and T_{mi} determine the optimal length, distal diameter, and the depth at which the prosthesis should be implanted. CI is a parameter that measures the ratio of the thickness of the inner and lateral cortices of the femoral isthmus to the transverse diameter of the femoral isthmus. Its clinical significance lies in fracture risk assessment and bone density evaluation. A higher CI indicates that the femur has greater structural strength, which may reduce the risk of fractures. When using certain prosthesis stems that require distal medullary cavity expansion, it is important to design an appropriate prosthesis and consider the thickness of the distal cortex to avoid femoral shaft fractures due to excessive expansion. The Cortical Index can serve as a certain reference for the degree of medullary cavity expansion.

The femoral stem needs to match the metaphyseal end of the femoral shaft, while CFI describes the shape of the entire proximal femur, and MCFI describes the shape of the metaphyseal medullary cavity, which is crucial for the design of the femoral stem prosthesis. In this experiment, the value of MCFI is 2.39. Chen et al. (23) emphasizes that the value of MCFI has a significant correlation with age. When designing a proximally fixed prosthesis, we should fully consider the impact of age factors.

5.3 Morphological parameters defined in our study

As shown in Figure 10, s_m shows a trend of first decreasing and then increasing. The position of the minimum value corresponds to the position of the isthmus. Combined with Tables 1, 5, the value of IH is 110.40 mm, and the value of LH is 446.96 mm. The ratio of IH to LH is calculated as 0.247, which is consistent with the ratio of 0.25 reported in the study by Chen et al. (23). Considering that the minimum often indicates the position of the isthmus, which plays an important role in guiding and limiting the placement of femoral prosthesis in clinical practice. Therefore, the isthmus is often used to

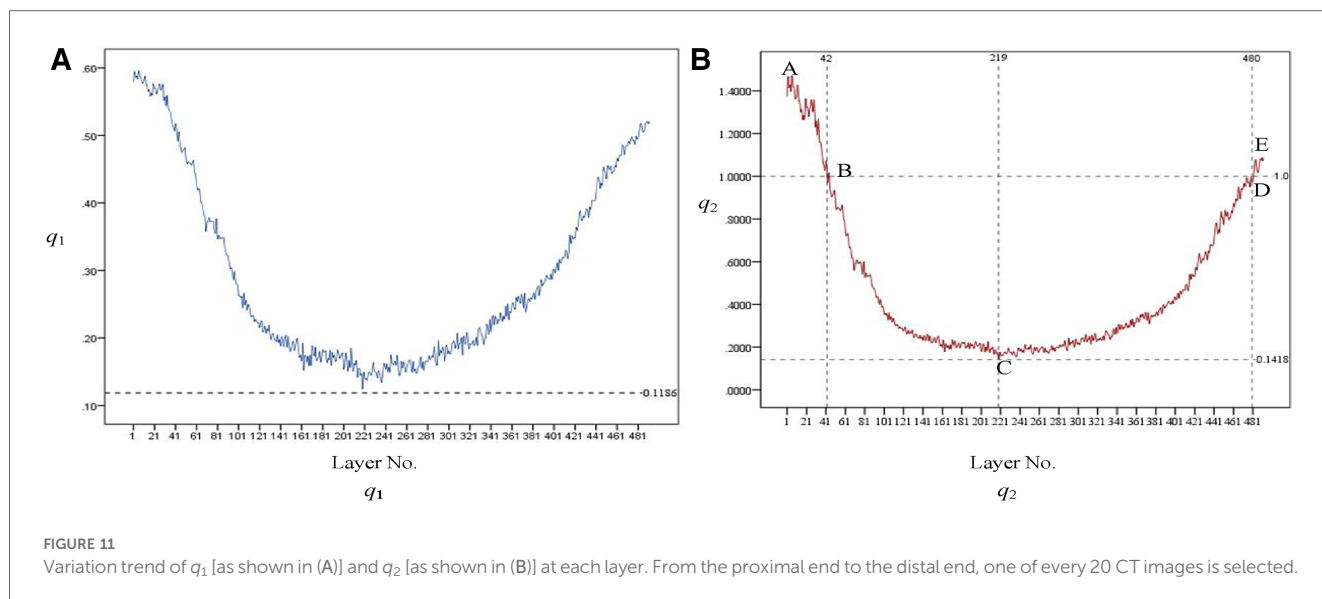


mark the warning farthest position of the femoral stem in its implantation of the medullary cavity. To ensure good fixation, the length of the femoral stem should be selected with due consideration of the isthmus position. For the patients in this study, the stem of the femoral prosthesis should extend up to 24.7% of the total length of the femur for optimal fixation.

The analysis of s_c has the following clinical significance. First of all, s_c provides the clinician with an indication of the expanding medullary. To stabilize the femoral stem prosthesis, medullary cavity expansion should be conducted with careful consideration of s_c at the isthmus to avoid puncturing the cortical bone. Secondly, s_c can be compared with the contralateral side during clinical diagnosis. If s_c is significantly lower than that of the healthy femur, it indicates a decrease in bone strength.

The variation trend of q_1 at each layer is shown in Figure 11A. An increase in q_1 indicates a tendency of medullary cavity enlargement, which significantly elevates the risk of fracture compared to that of normal healthy individuals. If there is an abundant data on healthy femoral bone marrow cavity, particular attention should be given to the average value of q_1 at the marker cross section C_{m0} , C_{m0-20} , C_{m0+20} , and C_{m1} . This can provide more robust data support for clinical diagnosis.

The variation trend of q_1 at each layer is shown in Figure 11B. q_2 initially exhibits a downward trend and then an upward one after passing the lowest point, C. At points B and D, q_2 equals 1, indicating that the area of the medullary cavity is equal to that of the cortical bone. s_m is larger than s_c on AB and DE and smaller than s_c on BD. This indicates that the proximal femoral cortex was thin in the bone and relatively thick in the isthmus. This suggests that, in the AB region, the thickness of the cortical bone is relatively small, and the medullary cavity is relatively large. Therefore, special attention should be given to the size of the



femoral stem prosthesis to prevent it from penetrating the cortical bone. The area near point C is the narrowest part of the medullary cavity. Thus, it is essential to consider the farthest accessible position and size of the distal end of the femoral stem prosthesis.

r_1 and r_2 indicate the growth rate of internal medullary cavity of the lesser trochanter and the upper femoral shaft, respectively. In this experiment, s_{m0+20} , s_{m0-20} , and s_{m1} was 3,313, 2,948, and 428, respectively. r_1 can be calculated as $r_1 = (3,313 - 2,948)/2,948 = 0.124$. r_2 can be calculated as $r_2 = (3,313 - 428)/428 = 6.74$. Therefore, during the design process of the femoral stem prosthesis, the narrowing of the femoral marrow cavity from proximal to distal should be fully considered.

5.4 Methods comparison

Measurement of femoral morphological parameters can be achieved through x-ray, CT scanning, and three-dimensional model reconstruction, each with its unique differences, advantages, and disadvantages. x-ray measurement is suitable for rapid screening and preliminary assessment, while CT scanning and three-dimensional model measurement are more appropriate for situations requiring precise measurement, such as preoperative planning. In our experiment, we employed a method that combines the use of Python

v3.3 and Mimics v15.0 for calculating medullary cavity parameters. Additionally, we utilized SPSS v24.0 for data analysis. In our study, by introducing randomness into the problem of solving the ROIMC, the method simplifies and accelerates the calculation of the morphological parameters. The advantage of this approach is that it provides a probabilistic model for analyzing the femoral medullary cavity, allowing for a more comprehensive and nuanced understanding of its morphology.

In addition, we added the parameters listed in Table 2. These parameters provide more detailed and precise anatomical information than traditional Noble. This helps to more accurately assess the morphology of the femur, allowing for a more personalized fit in the implant design. In addition, the three-dimensional parameters can better reflect the anatomical differences between individuals. Overall, our proposed morphological parameters provide more detailed and personalized information than the traditional Noble classification system, leading to improvements in orthopaedic implant design, surgical planning, and patient care.

The proposed method was compared to existing methods, as shown in Table 7. It was found that the research method presented in this paper is characterized by high degree of automation, simplicity, flexibility, and efficiency, considering the multi-dimensional information.

TABLE 7 Comparison between method presented and traditional method.

	Lin KJ (22)	Chen HX (23)	Yan L (24)	Pi YG (25)	Soodmand E (26)	Noble (39)	Our work
Femoral data	CT	x-ray	CT	x-ray	3D model	x-ray	CT
Measuring tool	Software of CT machine	PACS	Software of CT machine	Onis v2.3	Geomagic studio v10.0	Customized computer routines	Python v3.3 and Mimics v15.0
Analysis tools	Microsoft Excel	SPSS v20.0	SPSS v19.0	SPSS v18.0	/	BMDP Statistical Software	SPSS v24.0
Degree of automation	Low	Medium	Low	Medium	Medium	High	High
Whether to measure in multiple dimensions	No	No	No	No	No	No	Yes

6 Conclusion

Accurate and full utilization of anatomical information contained in femoral CT data is critical to improving the quality of personalized femoral stem design. Considering the deficiencies related to obtaining medullary cavity morphological parameters, a Monte Carlo-based method was proposed to in-depth measure and analyze the parameters of the femoral bone marrow cavity. The main contributions of this study were as follows.

- (1) By using Monte Carlo method, the problem of solving the ROIMC of the cross section of femoral marrow cavity without randomness was connected with a probability model to transform it into a problem of randomness. The results show that Monte Carlo-based method was simple and efficient to calculate the ROIMC of an irregular shape. It makes up for the lack of high-dimensional information acquisition in the existing medullary cavity morphological analysis
- (2) The measurement results of defined parameters a supplement to the existing parameters, and therefore provide more reasonable scientific basis for comprehensively understanding the anatomical morphological changes of the femoral marrow cavity. This has important significance and application to clinical practice. This method also provides a reasonable and reliable method for the prediction of bone related diseases, such as osteoporosis.

The experimental results showed that the proposed method was simple, flexible, and efficient, and can provide innovative ideas, methods, and techniques for other type of bones. The limitation of this study is that it does not establish a mapping relationship between the morphological parameters of the femoral marrow cavity and the prosthesis parameters of the hip joint. This relationship will be explored further in future work.

Data availability statement

The original contributions presented in the study are included in the article/Supplementary Material, further inquiries can be directed to the corresponding author.

Ethics statement

The studies involving humans were approved by the Ethics Committee of Xuzhou Medical University. The studies were conducted in accordance with the local legislation and institutional requirements. The participants provided their written informed consent to participate in this study. Written informed consent was

obtained from the individual(s) for the publication of any potentially identifiable images or data included in this article.

Author contributions

LW: Formal Analysis, Funding acquisition, Methodology, Writing – original draft, Writing – review & editing, Validation. HS: Formal Analysis, Software, Validation, Writing – original draft, Writing – review & editing. KG: Data curation, Formal Analysis, Funding acquisition, Writing – review & editing, Investigation. KH: Conceptualization, Formal Analysis, Funding acquisition, Writing – review & editing, Methodology. WG: Formal Analysis, Validation, Writing – original draft, Writing – review & editing. WZ: Software, Writing – review & editing. JW: Writing – review & editing.

Funding

The author(s) declare financial support was received for the research, authorship, and/or publication of this article.

This work was supported by National Natural Science Foundation of China (Grant No. 62102345), Natural Science Foundation of the Jiangsu Higher Education Institutions of China (Grant No. 19KJB520017), Natural Science Foundation of Jiangsu Province (Grant No. BK20201154), Talented Scientific Research Foundation of Xuzhou Medical University (Grant No. D2018017), Changzhou International Science and Technology Cooperation Project (Grant No. CZ20210038).

Conflict of interest

The authors declare that the research was conducted in the absence of any commercial or financial relationships that could be construed as a potential conflict of interest.

Publisher's note

All claims expressed in this article are solely those of the authors and do not necessarily represent those of their affiliated organizations, or those of the publisher, the editors and the reviewers. Any product that may be evaluated in this article, or claim that may be made by its manufacturer, is not guaranteed or endorsed by the publisher.

References

1. Pivec R, Johnson AJ, Mears SC, Mont MA. Hip arthroplasty. *Lancet*. (2012) 380 (9855):1768–77. doi: 10.1016/S0140-6736(12)60607-2
2. Kubicek J, Tomanec F, Cerny M, Vilimek M, Oczka D. Recent trends, technical concepts and components of computer-assisted orthopedic surgery systems: a comprehensive review. *Sensors*. (2019) 19(23):1–33. doi: 10.3390/s19235199

3. Mackenzie BN, Paul MW, Benjamin AL, Wayne EM, Samuel TK, David SJ. Examining the relationship between value and patient satisfaction with treatment in total joint arthroplasty. *Arthroplast Today*. (2024) 25:101311. doi: 10.1016/j.artd.2023.101311
4. Liu GA, Dai WF, Yu YY, Li GH. Research progress on the stability of prostheses in total hip arthroplasty. *Adv Clin Med*. (2024) 14(1):1789–95. (Chinese). doi: 10.12677/ACM.2024.141254
5. Naghavi SA, Hua J, Moazen M, Taylor S, Liu CZ. 3D fabrication of porous hip implant to reduce stress shielding and promote osseointegration. In: Mikos G, Fisher JP, editors. *Tissue Engineering Part A*. New Rochelle, NY, USA: Mary Ann Liebert, Inc (2022) 28. p. S536.
6. Macheras GA, Lepetos P, Galanakos SP, Papadakis SA, Poultsides LA, Karachalios TS. Early failure of an uncemented femoral stem, as compared to two other stems with similar design, following primary total hip arthroplasty performed with direct anterior approach. *Hip Int*. (2022) 32(2):166–73. doi: 10.1177/1120700020940671
7. Vala CH, Karrholm J, Kanis JA, Johansson H, Sten S, Sundh V, et al. Risk for hip fracture before and after total knee replacement in Sweden. *Osteoporos Int*. (2020) 31(5):887–95. doi: 10.1007/s00198-019-05241-x
8. Hartford JM, Knowles SB. Risk factors for perioperative femoral fractures: cementless femoral implants and the direct anterior approach using a fracture table. *J Arthroplasty*. (2016) 31(9):2013–8. doi: 10.1016/j.arth.2016.02.045
9. David K, Joseph R, Vinay A. Salvage options for the failed total knee arthroplasty. *Instr Course Lect*. (2024) 73:183–94.
10. Qiang Z, Cheng-Kung C, Hung-Wen W, Xiang D, Yi-Ting C, Yu-Shu L, et al. Biomechanical comparisons between a new avascular necrosis of femoral head stem based on Chinese patients with avascular necrosis and two other designs. *Chin Med J*. (2013) 126(10):1918–24. doi: 10.3760/cma.j.issn.0366-6999.20113248
11. Alamo JGD, Garcia-Cimbrello E, Castellanos V, Gil-Garay E. Radiographic bone regeneration and clinical outcome with the wagner SL revision stem: a 5-year to 12-year follow-up study. *J Arthroplasty*. (2007) 22(4):515–24. doi: 10.1016/j.arth.2006.04.029
12. Kelmer G, Stone AH, Turcotte J, King PJ. Reasons for revision: primary total hip arthroplasty mechanisms of failure. *J Am Acad Orthop Surg*. (2021) 29(2):78–87. doi: 10.5435/JAAOS-D-19-00860
13. Jiang N, Peng L, Al-Qwbani M, Xie GP, Yang QM, Chai Y, et al. Femoral version, neck-shaft angle, and acetabular anteversion in Chinese Han population: a retrospective analysis of 466 healthy adults. *Medicine (Baltimore)*. (2015) 94(21):e891. doi: 10.1097/MD.0000000000000891
14. Laumonerie P, Ollivier M, LiArno S, Faizan A, Cavaignac E, Argenson JN. Which factors influence proximal femoral asymmetry. *Bone Joint J*. (2018) 100(7):839–44. doi: 10.1302/0301-620X.100B7.BJJ-2017-1601.R1
15. Yang JY, Li Z, Zhan PY, Li XH, Wang KZ, Han JG, et al. Proximal femur parameter measurement via improved PointNet++. *Int J Med Robot*. (2023) 19(3):e2494. doi: 10.1002/rcs.2494
16. Jacquet C, Flecher X, Pioger C, Fabre-Aubrespy M, Ollivier M, Argenson JN. Long-term results of custom-made femoral stems. *Orthopedics*. (2020) 49(5):408–16. doi: 10.1007/s00132-020-03901-z
17. Liu Y, Zhang AB, Cai R, Chen H, Li C, Han Q, et al. Morphological measurement of the femoral anterior bow in Chinese population based on three-dimensional computed tomography. *BioMed Res Int*. (2021) 2021:7674764. doi: 10.1155/2021/7674764
18. Wuestemann T, Hoare SG, Petersik A, Hofstaetter B, Fehily M, Matsubara M, et al. Bone morphology of the proximal femoral canal: ethnicity related differences and the influence on cementless tapered wedge stem designs. *Hip Int*. (2021) 31(4):112070001989545. doi: 10.1177/1120700019895458
19. Zou RQ. *Measurement and Clinical Significance of the Diameter and Geometric Angle of the Upper Femoral Medullary Cavity in Normal Chinese Adults Using Three-Dimensional CT*. Jinan City: Shandong University of Traditional Chinese Medicine (2009). (Chinese).
20. Xue WD, Dai KR, Tang TT. Computer measurement method for the medullary cavity of the upper femur. *J Biomed Eng*. (2001) 18(2):303–5. (Chinese).
21. Uemura K, Otake Y, Sato Y, Takao M, Makino H, Soufi M, et al. Development of an open-source measurement system to assess the areal bone mineral density of the proximal femur from clinical CT images. *Arch Osteoporos*. (2022) 17(1):1–11. doi: 10.1007/s11657-022-01063-3
22. Lin KJ, Wei HW, Lin KP, Tsai CL, Lee PY. Proximal femoral morphology and the relevance to design of anatomically precontoured plates: a study of the Chinese population. *Sci World J*. (2014) 2014:1–6. doi: 10.1155/2014/106941
23. Chen HX, Shi NB, Xiong W, Peng YW, Peng HW, Li X. Measurement of anatomical parameters of medullary cavity based on stability of femoral end prosthesis and its clinical significance. *Chin J Anatomy*. (2019) 42(6):569–72. (Chinese).
24. Yan L, Xia J, Huang GY. Morphology analysis of the femoral canal in adult with developmental dysplasia of the hip. *Int J Osteol*. (2013) 34(5):368–70. (Chinese).
25. Pi YG. *The Measurement and Analysis of the Parameters in Relation to Proximal Femur of Chinese*. Changsha: Central South University (2012). (Chinese).
26. Soodmand E, Zheng GY, Steens W, Bader R, Nolte L, Klues D. Surgically relevant morphological parameters of proximal human femur: a statistical analysis based on 3D reconstruction of CT data. *Orthop Surg*. (2019) 11(1):135–42. doi: 10.1111/os.12416
27. Jacinto H, Valette S, Prost R. Multi-atlas automatic positioning of anatomical landmarks. *J Vis Commun Image Represent*. (2018) 50:167–77. doi: 10.1016/j.jvcir.2017.11.015
28. de Almeida DF, Ruben RB, Folgado J, Fernandes PR, Gamelas J, Verheghe B, et al. Automated femoral landmark extraction for optimal prosthesis placement in total hip arthroplasty. *Int J Numer Method Biomed Eng*. (2017) 33(8):e2844. doi: 10.1002/cnm.2844
29. David L, Luca M, Mónica B, Víctor E, Simo S. A survey of monte carlo methods for parameter estimation. *EURASIP J Adv Signal Process*. (2020) 2020(1):1–62. doi: 10.1186/s13634-020-0662-0
30. Braad PEN, Andersen T, Hansen SB, Høiland-Carlson PF. Strategies for CT tissue segmentation for Monte Carlo calculations in nuclear medicine dosimetry. *Med Phys*. (2016) 43(12):6507–16. doi: 10.1118/1.4967267
31. Kirby M, Morshed AH, Gomez J, Xiao PW, Hu YZ, Guo XE, et al. Three-dimensional rendering of trabecular bone microarchitecture using a probabilistic approach. *Biomech Model Mechanobiol*. (2020) 19(3):1–19. doi: 10.1007/s10237-020-01286-8
32. Eberlea R, Heinrich D, van den Bogert JA, Oberguggenberger M, Nachbauer W. An approach to generate noncontact ACL-injury prone situations on A computer using kinematic data of non-injury situations and Monte Carlo simulation. *Comput Methods Biomech Biomed Engin*. (2019) 22(1):3–10. doi: 10.1080/10255842.2018.1522534
33. Wang ZP, Li YP, Liang M, An SQ, Han YL. Adaptive monte carlo method for top-down assessment of measurement uncertainty. *Lab Med*. (2022) 37(4):382–6. doi: 10.3969/j.issn.1673-8640.2022.04.016
34. Wang L, He KJ, Chen ZM, Yang Y. A design method for orthopedic plates based on surface features. *J Mech Des*. (2017) 139(2):024502. doi: 10.1115/1.4035320
35. Wang L, He KJ, Chen ZM, Zou ZY, Xiang W. Serial design method for plates based on feature points mapping relation. *J Comput Aided Des Comput Graph*. (2016) 28(9):1587–97. (Chinese).
36. Wang L, He KJ, Chen ZM. Statistical analyses of femur parameters for designing anatomical plates. *Comput Math Methods Med*. (2016) 2016(2):1–12. doi: 10.1155/2016/1247560
37. Zuo JY, Zhang JG, Zhong T. Femoral edge contour connection algorithm based on canny detection. *J Shandong Univ Eng Ed*. (2015) 45(03):65–72. (Chinese).
38. Zhang M, Liu BL, Qi XZ, Yang QQ, Cheng CK. The three-dimensional morphology of femoral medullary cavity in the developmental dysplasia of the hip. *Front Bioeng Biotechnol*. (2021) 9:684832. doi: 10.3389/fbioe.2021.684832
39. Noble PC, Alexander JW, Lindahl LJ, Yew DT, Granberry WM, Tullos HS. The anatomic basis femoral component design. *Clin Orthop Relat Res*. (1988) 235:148–65. doi: 10.1097/00003086-198810000-00015
40. Ramme AJ, Vira S, Hotca A, Miller R, Welbeck A, Honig S, et al. A novel MRI tool for evaluating cortical bone thickness of the proximal femur. *Bull Hosp Joint Dis*. (2019) 77(2):115–21.
41. Rubin PJ, Leyvraz PF, Aubagniac JM. The morphology of the proximal femur: a three-dimensional radiographic analysis. *J Bone Joint Surg*. (1992) 74:28–32. doi: 10.2106/00004623-199274010-00005